Chapter 5

Conclusion

A fission chamber was built using U-233 coating to measure the charge of the emitted α-particles using the QADC. The triple GEM detector was build with a U-233 coating installed on the detector cathode to become sensitive to thermal and fast neutron fission reactions. The fission chamber performance was studied using the charge spectrum of the emitted α-particles from U-233 coating whose interactions are the closest to the heavily charged particles such as the fission fragments.

Increasing the size of the drift region increased the deposited charge in the drift. The height of the drift region increased to become 1 cm which increased the number of free electrons a 4.85 MeV α-particles to reach $(2.02 \pm 0.20) \times 10^5$ electron. Additionally, it helped in measuring α-particles of different energies. However, the difference in the deposited charge of the incident α-particles should be at least 27$\pm$ 11 pC when the fission chamber is operated at 2.87 kV and 3.57 kV for the GEM preamplifiers and the cathode respectively.

GEANT4 simulations were performed to calculate the charge of each emitted particle from U-233 coating in the drift region. In 90% Ar-gas and 10% /CO_2 gas mixture, ionization was main interaction in GEANT4 simulation that used in calculating the number of primary and secondary electrons in drift region. The α-particles produced the largest number of primary and secondary electrons compared to the other emitted particles in the drift region, and the number of free electrons for an α-particle whose energy was 4.85 MeV reached $(2.02 \pm 0.20) \times 10^5$ electrons.

GEANT4 simulated the number of free electrons in the drift region for β and γ-particles when the scattering process was included with the ionization. The number of free electrons was 100 electrons for β-particles of energy of exceeded 100 keV as predicted by GEANT4 and ESTAR software packages. In addition, each emitted photons from U-233 coating liberated a single free electron since their energies are within the photo-absorption limits. Therefore, the predicted contribution of β and γ-particles are negligible for a 100 keV β-particles and all the photons that might liberate photo-electrons within the same energy range. The prediction was dependent on the U-233 coating emission rate which is considered very low compared to those particles rates any neutron flux.

The measured charge spectrum by the QDC had two peaks, the first peak agreed with the simulated deposited charge of 4.85 MeV α-particles. The Garfield and GEANT4 simulation for the deposited charge of the 4.85 MeV α-particles in the drift region agreed with the first peak of a charge of 261$\pm$27 and a relative error of 9%. GEANT4 simulated was 2.02×10^5 free electrons liberated by ionization in the drift region, and then Garfield predicted the multiplication of the triple GEM preamplifiers which was $(8.81 \pm 2.5) \times 10^3$ electrons at 2.87 kV and 3.57 kV for the GEM preamplifiers and the cathode respectively.

The charge of the second peak agreed with GEANT4 and Garfield simulation for α-particles of energy of 6.40 MeV. The number of free electrons liberated by the 6.40 MeV was $(2.50 \pm 0.20) \times 10^5$ electrons which made the measured charge by the charge collector reached 353 ± 22 pC after electron multiplication. However, the U-233 α-particle spectrum measured by an α-spectrometer had only one main at 4.85 MeV. Additionally, the emission of 6.40 MeV is dependent on U-233 half-life that reaches 1.59×10^5 years.

The rate of each peak in the charge spectrum dropped after closing the FR4 shutter. The rate of the first peak reached to 0.32 Hz and the rate of the second peak reached 0.20 Hz. When the shutter is closed, both of them had a rate of 0.15 Hz confirmed that both peaks represented the charge of α-particles. Nevertheless, the difference in second peak rate was only 0.06 Hz, and the expected was to drop to half of the rate similar to the rate of the first peak. Thus, the second peak rate was independent on the FR4 shutter, and measured charge by the second peak was by the α-particles that were emitted with angle of 7 degrees as shown in Figure 5.1. The emitted α-particles within this 7 degrees had the longest track and deposited the highest charge in the drift region.

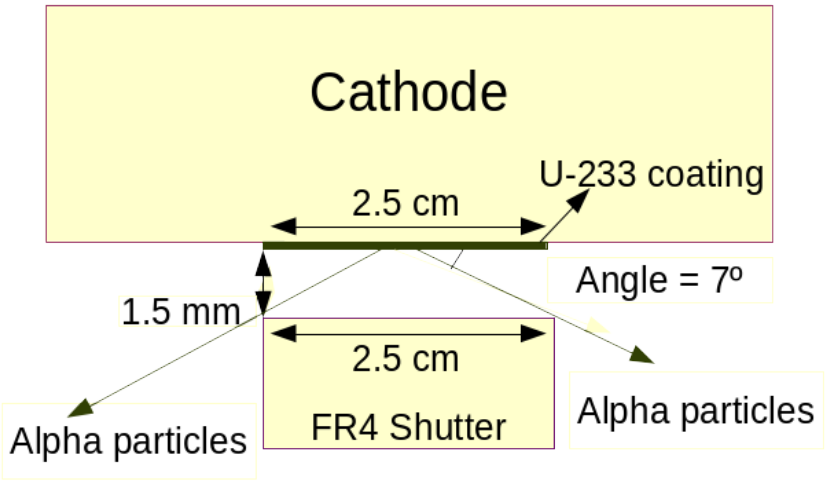

Figure 5.1: The emitted α-particles that avoid the FR4 shutter.

The predicted average charge carried by the signal of the light and heavy fission fragments after the GEM multiplication of $(8.81 \pm 2.5) \times 10^3$ electrons are 1.53×10^{12} and 7.13×10^{11} electrons respectively. Therefore, the detector is able to distinguish between light and heavy fission fragments. Although the fission chamber distinguish the type of the fission fragments, the gain of the fission chamber should be decreased to decrease the number of free electrons lower than Raether limit (10^8 electrons)[59] which will decrease the spark discharge probability in the fission chamber. Additionally, an advantage of a lower gain is increase the energy limit of low ionizing particles (photons and electrons) to contribute in the detector signal.

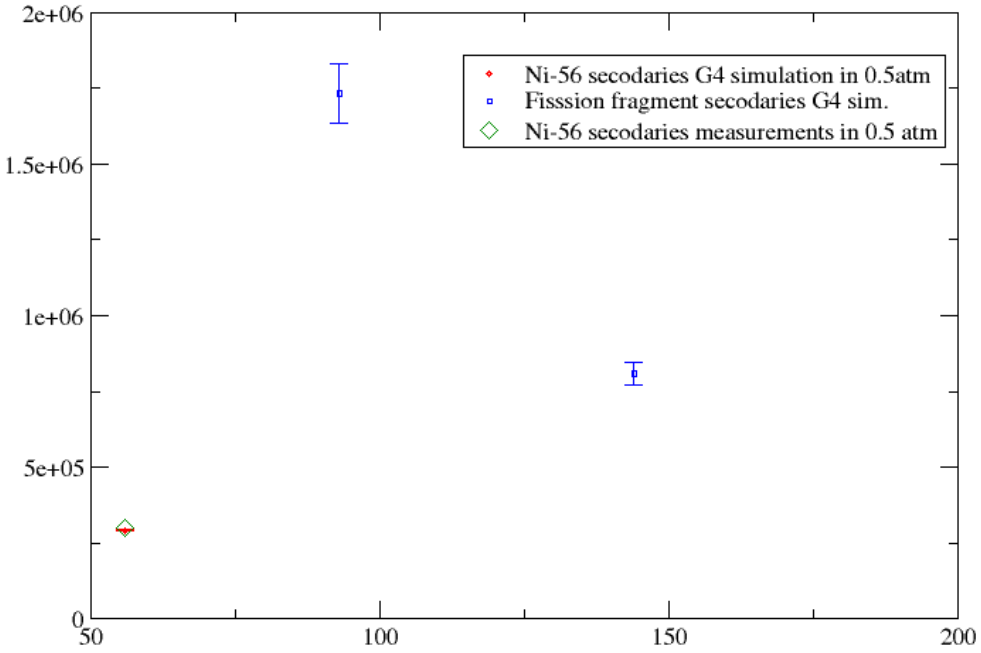

Figure 5.2: Simulation of the Secodary Electrons of Heavy and Light of U-233 Fission Fragments

References

[1] F. Sauli, et al, NIM A **386**, 531 (1997).

[2] G. Agocs, B. Clark, P. Martinego, R. Oliveira, V. Peskov,gand P. Picchi,JINST **3**, P020112, (2008).

[3] JP Holtzhausen, Dr WL Vosloo *High Voltage Engineering Practice and Theory*, ISBN: 978-0-620-3767-7.

[4] A.Bressan, et al, NIM A **424**, 321 (1999).

[5] Shalem Chen Ken, Master Thesis, Scientific Council of the Weizmann Institute of Science, 2005.

[6] Earl K. Hyde, *The Nuclear Properties of the Heavy Elements* (Academic,Denver Publications,1971).

[7] V.A Rykov, Atomic Energy **83**, 1 (1997).

[8] J.M. valentine, C.Curran, Reports on Progress in Physics **21**, 1 (1958).

[9] IAEA INDC(BLR)-016, Printed by the IAEA in Austria, 2003.

[10] IAEA STI/PUB/1291, Printed by the IAEA in Austria, 2007.

[11] R.Chechik,A.Breskin,C.Shalem, NIM A **535**, 303 (2004).

[12] Bondar,A.Buzulutskov,A.Grebernuk, JINST **3** P07001 (2008).

[13] William R. Leo, *Techniques for Nuclear and Particle Physics Experiments* (Springer-Verlag,1995).

[14] D. C. Biswas, M. N. Raob and R. K. Choudhury,NIM B **53**, 3, 251(1991).

[63] A.Sharma,F. Sauli, CERN PPE/93-50, 1993.

[16] M. Facina, Master Thesis, Leuven, 2004.

[17] J.C.Hudler, Radiation Measurements **43**, S334 (2008).

[18] Syed Ahmed, Physics and Engineering of Radiation Detection (Academic Press 2007).

[19] R. Chechik, A. Breskin, G. P. Guedes, D. Mrmann, J. M. Maia, V. Dangendorf, D. Vartsky, J. M. F. Dos Santos, and J. F. C. A. Veloso, Recent Investigations of Cascaded GEM and MHSP detectors, IEEE Trans. Nucl. Sci., 51,5, (2004)

[20] Physik Department E18, Technische University Munchen, 2D readout Plane, 21 of Jun.2012.

[21] Particle Data Group, Particle Physics Booklet, July 2008

[22] treetman, Ben, Banerjee, Sanjay, Solid State Electronic Devices, Fifth Edition

[23] Pinto, Serge . Gas Electron Multipliers Development of large area GEMS and spherical GEMS. Diss. Mathematisch-Naturwissenschaftliche Fakultt , 2011

[24] Akovali, Y. (1990, January 1). Table of Radioactive Isotopes. Retrieved January 1, 2014.

[25] Fabio, S. (2014). Basic processes in gaseous counters. In Gaseous Radiation Detectors: Fundamentals and Applications. Cambridge: University Printing House

[26] Saito, K., Sasaki, S. (2003). Simultaneous Measurements of Absolute Numbers of Electrons and Scintillation Photons Produced by 5.49 MeV Alpha Particles in Rare Gases. IEEE TRANSACTIONS ON NUCLEAR SCIENCE, 50(6), 2452-2460

[27] Agostinelli, S. (2003). Geant4a simulation toolkit. Nuclear Instruments and Methods in Physics Research Section A: Accelerators, Spectrometers, Detectors and Associated Equipment, 506(3), 250303

[28] Ziegler, J. (2010). SRIM - The stopping and range of ions in matter (2010). Nuclear Instruments and Methods in Physics Research Section B: Beam Interactions with Materials and Atoms, 268(11-12), 1818-1823

[29] Hanke, C., Bichsel, H. (1970). Precision energy loss measurements for natural alpha particles in argon. Kbh.: Det Kongelige Danske Videnskabernes Selskab

[30] Garfieldpp. (n.d.). Retrieved June 1, 2013,from http://garfieldpp.web.cern.ch/garfieldpp.

[31] HEED. (n.d.). Retrieved June 1, 2013,http://ismirnov.web.cern.ch/ismirnov/heed

[32] WNA. (2014, December 1). Uranium and Depleted Uranium. Retrieved May 1, 2015. from http://www.world-nuclear.org/info/Nuclear-Fuel-Cycle/Uranium-Resources/Uranium-and-Depleted-Uranium/

[33] LANL. (n.d.). Index to ENDF/B-VII.1 Decay Data. Retrieved May and June, 2015, from https://t2.lanl.gov/nis/data/endf/decayVII.1.html

[34] ESTAR. (n.d.). Stopping Power. Retrieved May 1, 2015, from http://physics.nist.gov/PhysRefData/Star/Text/ESTAR.html

[35] Raju, G. (2004). Electron-atom Collision Cross Sections in Argon: An Analysis and Comments. IEEE Transactions on Dielectrics and Electrical Insulation, 11(4), 649.

[36] Sauli, F. (1977). Principles of operation of multiwire proportional and drift chambers. Retrieved May 15, 2015, from http://cds.cern.ch/record/117989

[37] Binnie, D. (1985). Drift and diffusion of electrons in argon/CO2 mixtures. Nuclear Instruments and Methods in Physics Research A, 234, 54-60.

[38] Uranium and Depleted Uranium. (2014). Retrieved May 1, 2015, from http://www.world-nuclear.org/info/Nuclear-Fuel-Cycle/Uranium-Resources/Uranium-and-Depleted-Uranium/

[39] nunziata, M. (2012). Handbook of radioactivity analysis (3rd ed.). San Diego: Academic Press.

[40] IAEA. (2003). Manual for reactor produced radioisotopes. Vienna: IAEA.

[41] Reuss, P. (2008). Neutron physics. Les Ulis, France: EDP Sciences.

[42] Jurado, M.,Fernandez,A., (2005). Dependence of self-absorption on thickness for thin and thick alpha-particle sources of UO2. Nuclear Instruments and Methods in Physics Research A, 548, 432438.

[43] Gorbachev, V., and Zamiatnin, I. (1980). Nuclear reactions in heavy elements: A data handbook. Oxford: Pergamon Press.

[44] Stein, W. (1957). Velocities of Fragment Pairs from U-233, U-235, and Pu-239 Fission. Physical Review, 94-98.

[45]

[46] ANSYS Academic Research, Release 15.0

[47]

[48] Knief R.A., (1992). Nuclear Engineering: Theory and Technology of Commercial Nuclear Power. 2nd ed. e.g. England: Hemisphere Publishing Corporation.

[49] ROOT — A Data Analysis Framework. (n.d.). Retrieved June 25, 2009, from https://root.cern.ch/drupal/

[50] Shekhtman, L., Aulchenko, V., Bondar, A., Dolgov, A., Kudryavtsev, V., Nikolenko, D., . . . Zhulanov, V. (2012). GEM-based detectors for SR imaging and particle tracking. J. Inst. Journal of Instrumentation.

[51] Carron, N. (2007). An introduction to the passage of energetic particles through matter. Boca Raton: Taylor and Francis.

[52] Belic, D., Lecointre, J., and Defrance, P. (2010). Electron impact multiple ionization of argon ions. Journal of Physics B: Atomic, Molecular and Optical Physics, 185203-185203.

[53] ahin, , Tapan, I., zmutlu, E., and Veenhof, R. (2010). Penning transfer in argon-based gas mixtures. J. Inst. Journal of Instrumentation.

[54] Zuydtwyck, D. (2010). Development of micro-pattern gaseous detectorsgem. (master's thesis).

[55] Annunziata, M. (2003). Handbook of Radioactivity Analysis (Second Edition). Academic Press.

[56] Huxley, L., and Crompton, R. (1974). The diffusion and drift of electrons in gases. New York: Wiley.

[57] Mason, E., and McDaniel, E. (1988). Transport properties of ions in gases. New York: Wiley

[58] ENSDF Decay Data in the MIRD Format for 233Pa. (n.d.). Retrieved August 7, 2015.

[59] Raizer, Y., and Kisin, V. (1991). Gas discharge physics. Berlin: Springer Verlag.

[60] Chabod, S., Fioni, G., Letourneau, A., and Marie, F. (2006). Modelling of fission chambers in current modeAnalytical approach. Nuclear Instruments and Methods in Physics Research Section A: Accelerators, Spectrometers, Detectors and Associated Equipment, 633-653.

[61] Kuffel, E., and Zaengl, W. (2000). High voltage engineering fundamentals (2nd ed.). Oxford: Butterworth-Heinemann/Newnes.

[62] Biagi, S. (n.d.). Http://magboltz.web.cern.ch/magboltz/. Retrieved September 1, 2015

[63] A.Sharma,F. Sauli, first Townsend coefficients measurements for argon gas european organization for nuclear research (1993).

[64] Jungwirth, M., Breitkreutz, H., Wagner, F., and Bcherl, T. (2012). Determination of the photon spectrum in an intense fission neutron beam. J. Inst. Journal of Instrumentation.

[65] ORTEC. (n.d.). ORTEC 928. Retrieved from http://www.ortec-online.com/download/926-MNL.pdf

[66] Franck, J. (2015). GEM Tracking Detectors for COMPASS. Retrieved October 1, 2015, from https://www.e18.ph.tum.de/research/compass/gempixelgem-tracking-detectors/

[67] CERN - European Organization for Nuclear Research - Physics Department - DT. (n.d.). Retrieved October 15, 2012, from http://rd51-public.web.cern.ch/RD51-Public/

[68] Documentation. (n.d.). Retrieved October 25, 2015, from http://garfieldpp.web.cern.ch/garfieldpp/documentation

[69] GEANT4 physics manual. (2014, December 1). Retrieved September 25, 2015, from http://geant4.web.cern.ch/geant4/UserDocumentation/UsersGuides/PhysicsReferenceManual

[70] Kahn, B. (2007). Radioanalytical chemistry. New York: Springer

[71] R. Dunker, Environmental lab quantitaties data, August 2015.

Appendix A

Solving Boltzmann Eqaution

A.1 Solving Boltzamn Equation for a Hole of Uniform Electric Field [56]

Asymptotic solution details for Boltzmann Equation A.1 for a hole has a uniform electric field takes the form in Equation A.2.

$$D(\frac{\partial^2}{\partial x^2}+\frac{\partial^2}{\partial x^2})n + D_L\frac{\partial^2}{\partial z^2} - W\frac{\partial}{\partial z}n = 0 \tag{A.1}$$

$$n(x', y', z') = e^{\lambda_L z'}V(x, y, z) \tag{A.2}$$

$$\nabla'^2 V = \lambda_L^2 V \tag{A.3}$$

$$\nabla'^2 V = \frac{\partial^2}{\partial x'^2}+\frac{\partial^2}{\partial y'^2}+\frac{\partial^2}{\partial z^2} \tag{A.4}$$

$$x' = \frac{D_L}{D}xy' = \frac{D_L}{D}y \tag{A.5}$$

Using spherical coordinates, Equation A.3 as be written as in Equation A.6 which is symmetric in ϕ direction.

$$\frac{1}{r'^2}\frac{\partial}{\partial r'}r'^2\frac{\partial V}{\partial r'}+\frac{1}{r'^2 sin\theta'}\frac{\partial}{\partial\theta}sin\theta\frac{\partial V}{\partial\theta} = \lambda_L^2 V \tag{A.6}$$

Assuming $V(r', \theta) = R_k(r')P_k(\mu)$ the solution of the zenith angle direction is the Legendre polynomial, and can be written as shown in the Equation A.7.

$$\frac{1}{r' sin\theta}\frac{\partial}{\partial\theta}sin\theta\frac{\partial V}{\partial\theta} = R_k(r')\frac{d}{d\mu}\left[(1-\mu^2)\frac{dP_k(\mu)}{d\mu}\right] \tag{A.7}$$

and

$$\frac{d}{d\mu}\left[(1-\mu^2)\frac{dP_k(\mu)}{d\mu}\right] = -k(k+1)P_k(\mu) \tag{A.8}$$